A Monte Carlo simulation of the time-of-flight experiment in non-uniformly defected thin crystalline layers

1995 J. Phys.: Condens. Matter 7 2987

(http://iopscience.iop.org/0953-8984/7/15/006)

J. Phys.: Condens. Matter 7 (1995) 2987–2999. Printed in the UK

A Monte Carlo simulation of the time-of-flight experiment in non-uniformly defected thin crystalline layers

J Rybicki†§, A Rybicka†§, S Feliziani†, G Mancini† and M Chybicki‡

† Istituto di Matematica e Fisica, Università di Camerino, Camerino (MC), Italy

‡ Faculty of Technical Physics and Applied Mathematics, Technical University of Gdańsk, Narutowicza 11/12, 80-952 Gdańsk, Poland

Received 24 October 1994, in final form 17 January 1995

Abstract. In the present paper we report on the results of the Monte Carlo simulation of the time of flight (TOF) experiment for r and r–ε hopping transport in highly defected very thin crystalline layers. The defects are considered as localized states, between which a hopping motion of the injected carriers is possible. The total (integrated over energy) density of defects is assumed to be spatially non-uniform on the macroscopic scale, i.e. the scale comparable with the layer thickness. In particular, we consider an exponential dependence of the total density of hopping centres on the distance from the layer contacts. The results of simulations performed for various defect concentrations, various defect distributions in energy, and various degrees of the layer spatial non-uniformity are discussed. It is shown that both r and r–ε hopping transient currents measured in the classical TOF experiment are highly sensitive to the spatial macroscopic scale variations of the total centre concentration. The detailed shape of the transients depends in a complicated way on the system dilution, the energetic centre distribution, and the character of the spatial variations of the total centre density. The existence of the spatial non-uniformity of the layer could be recognized experimentally by observation of the qualitative changes of the current shape with increasing temperature, which leads to lower dispersion, and thus more pronounced characteristic features of the x-dependent total centre density, such as a higher polarity dependence, or the appearance of the current maxima or plateaux just before the effective TOF.

1. Introduction

One of the classical method for determination of the microscopic transport parameters is the analysis of the results obtained in the time of flight (TOF) experiment (see, e.g., Marshall 1983a, Marshall and Main 1983, Marshall *et al* 1985, Weissmiller 1985, Muller-Horsche *et al* 1987, Di Marco *et al* 1989, Seynhaeve *et al* 1988). In this experiment an infinitesimally thin sheet of charge carriers is produced near one of the surfaces of a thin layer placed between two contacts, and subject to an external electric field. The subsequent motion of the carriers towards the collecting contact results in a transient current, which is analysed in an external circuit connected to the sample. The theory of the TOF experiment (Scher and Montroll 1975, Schmidlin 1977a, b, Arkhipov and Rudenko 1982, Rudenko and Arkhipov 1982a, b) permits us to perform an extensive analysis of the transient currents measured in the macroscopically uniform layers. However, a number of phenomena can introduce the macroscopic scale variations of the total density of traps or hopping centres over the

§ Permanent address: Faculty of Technical Physics and Applied Mathematics, Technical University of Gdańsk, Narutowicza 11/12, 80-952 Gdańsk, Poland.

0953-8984/95/152987+13$19.50

layer thickness (see, e.g., Kao and Hwang 1981 p 150, Samoć and Zboiński 1978), which can be of crucial importance in the case of very thin layers. Thus, a straightforward application of the theory developed for spatially uniform layers cannot be reliable. For the multiple-trapping transport mechanism (i.e. a band transport interrupted by trapping events; a temporarily immobilized carrier is thermally re-emitted into the conduction band) the influence of the spatial non-uniformity in the trap distribution on the transient currents, measured in the constant-temperature TOF experiment, as well as in the thermally stimulated TOF experiment, has been investigated by Rybicki and Chybicki (1988, 1989), Rybicki *et al* (1990, 1991b), and Tomaszewicz *et al* (1990), and some simple formulas for determination, or at least estimation, of the spatial distribution of the multiple-trapping centres have been proposed. The TOF transient currents are intensively studied also in materials that reveal a hopping mechanism of transport (carrier tunnelling or thermally activated tunnelling between localized states; see, e.g., Emoto and Kotani 1983, Bassler *et al* 1982, Bassler 1984, Schein *et al* 1986, Yuh and Stolka 1988, Abkowitz *et al* 1989). The measurement interpretation for the hopping transport mechanism is more difficult than in the case of multiple-trapping transport, and computer experiments (Monte Carlo simulations) are often performed in order to elucidate certain features of the hopping transport in materials characterized by diagonal and/or off-diagonal disorder (see, e.g. Adler and Silver 1982, Marshall 1978, 1981, 1983b, Marshall and Sharp 1980, Ries and Bassler 1987, Pautmeier *et al* 1989, Richert *et al* 1989 (in macroscopically uniform layers) Rybicki *et al* 1992, 1993 (in macroscopically non-uniform amorphous layers)).

In the present paper we deal with the influence of a spatial non-uniformity of the macroscopic scale hopping centre distribution on the TOF transient currents in the case of crystalline materials. In section 2 we describe in brief the Monte Carlo algorithm we have applied. The simulation results showing the TOF transient currents in their dependence on various model spatial and energetic distributions of hopping centres $N_h(x, \varepsilon)$ are presented and discussed in section 3. Section 4 contains concluding remarks.

2. The simulation algorithm

We consider a thin layer of thickness L placed between two planar contacts (one at $x = 0$ and one at $x = L$) with an x-dependent total density of hopping centres. At $t = 0$ an infinitesimally thin sheet of carriers is generated on the left contact ($x = 0$). The applied external electric field E enforces the carrier motion towards the $x = L$ contact. The field E is held constant and uniform, so that no space charge effects are included. The transport mechanism to be considered is r–ε hopping, i.e. hopping between defects, acting as hopping centres, and distributed at random in energy ε, according to a given distribution $f(\varepsilon)$, and at random over the crystal lattice, with a total local concentration $N_0 S(x)$, where $S(x)$ is a rather slowly varying function of x. The centre distribution can be thus written in the factorized form as

$$N_h(x, \varepsilon) = N_0(D) S(x; D) f(\varepsilon) \tag{1}$$

where the energetic distribution $f(\varepsilon)$ is normalized:

$$\int_{-\infty}^{\infty} f(\varepsilon)\, d\varepsilon = 1$$

and $S(x; D)$ is in general a one-parameter (D) family of x-dependent functions, describing the spatial variations of the total local centre density. The particular form of $S(x; D)$ used in

this work will be specified in the end of the section. $N_0(D)$ is a D-dependent normalization factor chosen in such a way that

$$\frac{1}{L}\int_0^L N_0(D)S(x;D)\,\mathrm{d}x$$

does not depend on D, and is the total number of centres in the layer per unit surface of the contact. The simple functional form of (1) imposes a strong limitation on possible centre distributions in space and in energy, e.g. excluding from our considerations the case of interacting defects, where $f(\varepsilon)$ could depend on the total local centre density $N_0(D)S(x;D)$. However, the factorized expression (1) is sufficiently flexible to cover a rather wide range of possible centre distributions in x and ε. The simulation system is similar to that used by Ries and Bassler (1987): a regular cubic lattice containing $70 \times 50 \times 50$ sites with periodic boundary conditions imposed in directions perpendicular to the applied field. A fraction c of the total number of the lattice nodes is chosen as hopping centres, and distributed along the direction of the external field E according to $S(x;D)$. The energies taken from the normalized distribution $f(\varepsilon)$ are then assigned to the transport sites. The remaining fraction $1-c$ of the lattice nodes is labelled as host sites not participating in the transport process.

The transient currents were calculated from the time and spatial evolution of the injected carrier packet $n(x,t)$ during its motion towards $x = L$, according to the expression

$$j(t) = -\frac{1}{n_0}\frac{\mathrm{d}}{\mathrm{d}t}\left(\int_0^L n(x,t)\,\mathrm{d}x\right) + \frac{1}{n_0 L}\frac{\mathrm{d}}{\mathrm{d}t}\left(\int_0^L xn(x,t)\,\mathrm{d}x\right) \tag{2}$$

(see, e.g., Leal Ferreira 1977), where $j(t)$ is the particle current per carrier and n_0 is the total number of injected carriers. The applied increment of $\log t$ was equal to 0.1 or 0.05. The carrier packets $n(x,t)$ were obtained by averaging the random walks of 3000 individual carrier (20 carriers for each of 150 site generations). The random walk of each individual carrier was started at $x = 0$ and $t = 0$, and finished on arriving to the collecting electrode at $x = L$.

An individual hop from a given occupied centre, say at r_0, to one of the neighbouring empty centres, located at r_i, $i = 1, \ldots, 342$ (from a $7 \times 7 \times 7$ cube centred on r_0), has been realized as follows. The average jump rate ν_{0i} of the hop from the centre at r_0 to the ith neighbour at r_i is given by (see, e.g., Ries and Bassler 1987)

$$\nu_{0i} = \begin{cases} \nu_0 \exp(-2\alpha|r_0 - r_i|)\exp(-\Delta U_{0i}/kT) & \Delta U_{0i} > 0 \\ \nu_0 \exp(-2\alpha|r_0 - r_i|) & \Delta U_{0i} \leqslant 0 \end{cases} \tag{3}$$

where

$$\Delta U_{0i} = \varepsilon_i - \varepsilon_0 - qE(x_i - x_0). \tag{4}$$

According to the average jump rates ν_{0i} (3)–(4), random jump rates ν_i are chosen from an exponential distribution. The probability p_i of the jump to the ith centre is given by

$$p_i = \nu_i \Big/ \sum_{i=1}^{n} \nu_i \tag{5}$$

and the most probable jump is accepted in the simulations. In equations (3)–(5), α is the reciprocal Bohr radius, ε_0 and ε_i are the energies of the actually occupied centre and the

ith neighbouring unoccupied centre, ν_0 is the frequency factor, q is the elementary charge, T is the temperature, and k is the Boltzmann constant.

Let us now specify the function $S(x; D)$ and $f(\varepsilon)$ from (1). In order to investigate qualitatively the influence of the macroscopic non-uniformity of the spatial centre distribution, we performed our simulations for exponential variations of the centre concentration in the function of x. Such a spatial distribution of hopping centres corresponds to diffusive, or radiative, origin of the defects. In particular, the results presented in the following section were obtained for

$$S(x; D) = \exp(-x/D) \tag{6}$$

and

$$S(x; D) = \exp(-(L - x)/D) \tag{7}$$

where D is a concentration decay (increase) parameter. The degree of the layer non-uniformity may be conveniently expressed as L/D. $L/D = 0$ corresponds to the uniform spatial distribution. As far as the energetic centre distribution $f(\varepsilon)$ is concerned, we used the normalized Gaussian distribution of half width σ/kT. For σ/kT close to zero we have a discrete energy level, which corresponds to r hopping (nearest-neighbour hopping).

The simulations have been performed for the systems with various values of the parameters in the following ranges: average total concentration c of hopping centres, $0.1 \leqslant c \leqslant 1.0$; half width σ of the Gaussian distribution in energy, $0.0 \leqslant \sigma \leqslant 7.0kT$; spatial non-uniformity parameter L/D, $0.0 \leqslant L/D \leqslant 3.0$. The parameters common to all the simulations are (cf Ries and Bassler 1987) a cubic lattice constant $d = 7 \times 10^{-10}$ m, a wave-function overlap parameter $2d\alpha = 5.0$, where α is the reciprocal Bohr radius, a temperature $T = 400$ K, and an external electric field $E = 1.1 \times 10^8$ V m^{-1}. The time is normalized to $1/\nu = \tau$, where $\nu = 6\nu_0 \exp(-2d\alpha)$. τ is the average dwell time of a carrier located at a site of an undiluted ($c = 1.0$) cubic lattice with six nearest neighbours.

3. Simulation results

Prior to presenting the influence of the spatial macroscopic scale non-uniformity of the total centre concentration on the r and r–ε hopping TOF signals (subsections 3.2 and 3.3), we shall show separately the pure effects of decreasing total centre concentration, and increasing width of the Gaussian energetic distribution, in spatially uniform layers (subsection 3.1, cf Ries and Bassler 1987).

3.1. Spatially uniform layers

In figure 1 we show several transient currents calculated from (2) for the x-independent (constant over the layer thickness) average spatial centre density without any energetic disorder (figure 1(A)), which corresponds to the nearest-neighbour hopping (r hopping), and with centres distributed in energy according to the Gaussian distribution (figure 1(B) and (C)), which corresponds to the variable-range hopping (r–ε hopping). In each figure the only parameter being changed is the average centre concentration c. Figure 2 shows the histograms of the numbers of jumps performed by the carriers during their random walk from $x = 0$ to $x = L$. As is seen from figure 2, dispersion of the total numbers of hops increases rapidly with decreasing site concentration c, and also with increasing width of

the energetic distribution σ, in accordance with the increasing dispersive character of the transients in figure 1. Initial slopes $1-\alpha$ of the r–ε hopping transient currents in spatially uniform layers obey only approximately the formula of Schonherr *et al* (1980), which reads $\alpha^{-1} = (\sigma/4\sqrt{2}kT)^2 + 1$, and does not predict any dependence of the slope on c. The slopes $1-\alpha$ obtained in our simulations depend on the site concentration c. The best agreement with the mentioned formula is found for $c \approx 0.5$ ($\approx 2\%$); for higher (lower) concentrations the slopes are smaller (greater) than predicted by Schonherr *et al* (1980) (by $\sim 10\%$ for $c = 1.0$ and $c = 0.1$). The slopes $1+\beta$ of the final current decay decrease on decreasing defect concentration, and/or on increasing width of the centre distribution in energy (cf figure 7(A) below).

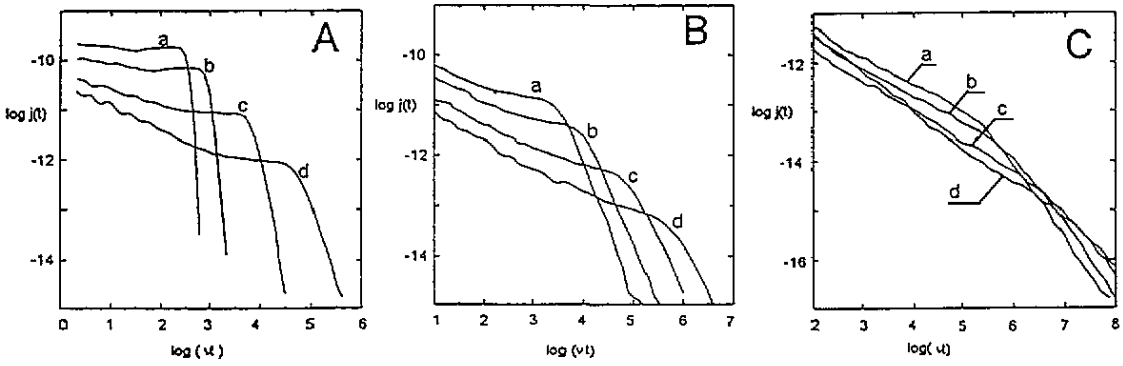

Figure 1. Transient currents for various hopping centre concentrations c for spatially uniform systems: curves a, $c = 1.0$; curves b, $c = 0.5$; curves c, $c = 0.2$; curves d, $c = 0.1$; (A) $\sigma = 0.0kT$; (B) $\sigma = 3.5kT$; (C) $\sigma = 7.0kT$.

3.2. Spatially non-uniform layers—current profiles

Let us turn to the influence of the spatial non-uniformity of the centre distribution on the reference TOF transient currents shown above. For the spatial centre distribution (6) the hopping carriers moving towards $x = L$, with increasing x, enter a region of lower centre density, and thus their motion is slowed down. For the spatial centre distribution (7), the centre density increasing with x makes the carrier motion easier near the collecting electrode. Figure 3 shows typical spatial distribution $n(x,t)$ of hopping carriers at the same time ($\nu t = 10^4$) after the injection into the layer with a given concentration c ($c = 0.2$), for the centre concentration increasing and decreasing e^3 times over the layer thickness (○ and ● respectively), and also for a uniform spatial centre distribution (▽). Figure 3(A) refers to r hopping ($\sigma = 0.0kT$), figure 3(B) to r–ε hopping (with $\sigma = 3.5kT$). For spatial distribution (7), the carriers begin their random walk in the low-concentration region, and spend a relatively (in respect to the effective TOF) long period of time in the immediate proximity of the injecting contact. Due to the presence of deep tail centres in the case of r–ε hopping, up to the given moment of time, the carrier packet for $\sigma = 0.0kT$ (figure 3(A)) has penetrated a longer distance from $x = 0$ than the packet with $\sigma = 3.5kT$ (figure 3(B)). For the uniform spatial centre distribution (▽), the considered time $\nu t = 10^4$ is somewhat greater than the effective TOF for r hopping (figure 3(A); cf curve c in figure 1(A)), and within the sample only few carriers remain (note a logarithmic scale on the vertical axis). For r–ε hopping, $\nu t = 10^4$ remains well below the effective TOF (cf curve c in figure 1(B)) and we can see a well developed carrier packet. For spatial distribution (6), the carriers

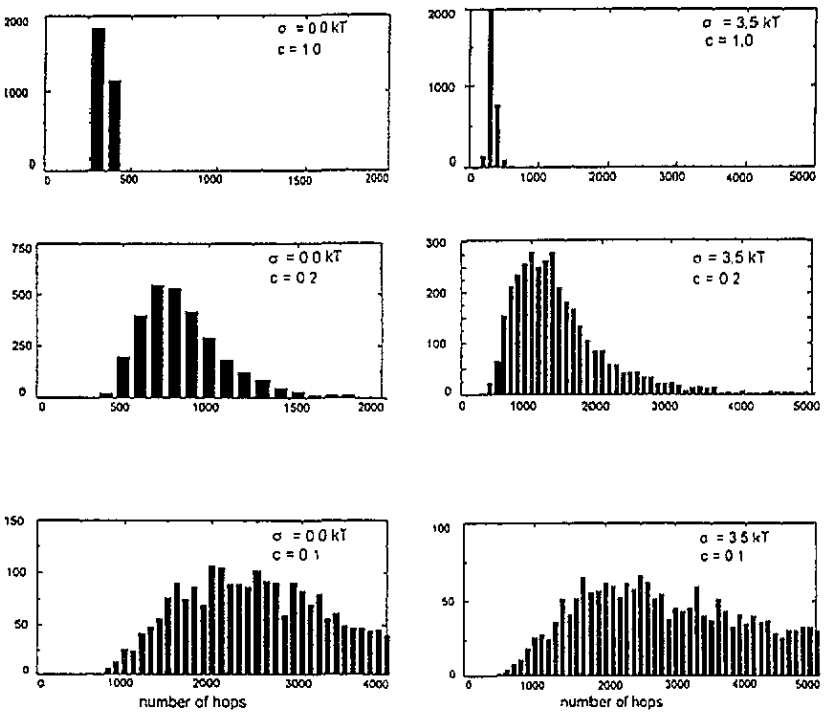

Figure 2. Histograms of the total numbers of jumps performed by the carriers during their walk from $x = 0$ to $x = L$, for concentrations $c = 1.0$, 0.2, and 0.1, and for energetic distribution half width $\sigma = 0.0kT$ (r hopping) and $\sigma = 3.5kT$ (r–ε hopping). The heights of the columns correspond to the numbers of carriers that performed given numbers of hops. The histogram resolution is 100 hops. The average hopping centre density is uniform over the layer thickness.

begin their random walk in the high-concentration region, and within a relatively short time leave the region close to the injecting contact. The carrier packets remain then for a relatively long time in the central part of the layer, trying to penetrate the low-concentration region near $x = L$. Such a behaviour of the carrier packets has a remarkable influence on the TOF current profiles. Figures 4–6 show the influence of the degree of the layer spatial non-uniformity L/D on the currents for $c = 0.5$, 0.2, and 0.1.

Let us consider first the case of decreasing total concentration of hopping centres (6). The initial value of the current obviously depends on the actual ratio L/D, because the number of hopping centres on the injecting contact ($x = 0$) is different for different values of L/D. With increasing degree of non-uniformity, L/D, the average slopes before the effective TOF increase, and thus, roughly speaking, the increase of L/D acts qualitatively like a decrease of the centre concentration c, and/or an increase of the energetic distribution width σ. However, there is an important difference in temporal variations of the current slope. In uniform structures the current initially decays more rapidly than just before the effective TOF (figure 1), due to the carrier relaxation in energy (Ries *et al* 1988, Pautmeier *et al* 1989). In contrast, in sufficiently non-uniform layers (for the parameters used here $L/D \geqslant 1$) with a total centre concentration decreasing with increasing x, the effect is dominated by the influence of increasing (with x) average distance between the transport sites, and the current profile is steeper immediately before the TOF than at much shorter times, when the most rapid carrier relaxation in energy occurs. After the effective TOF the

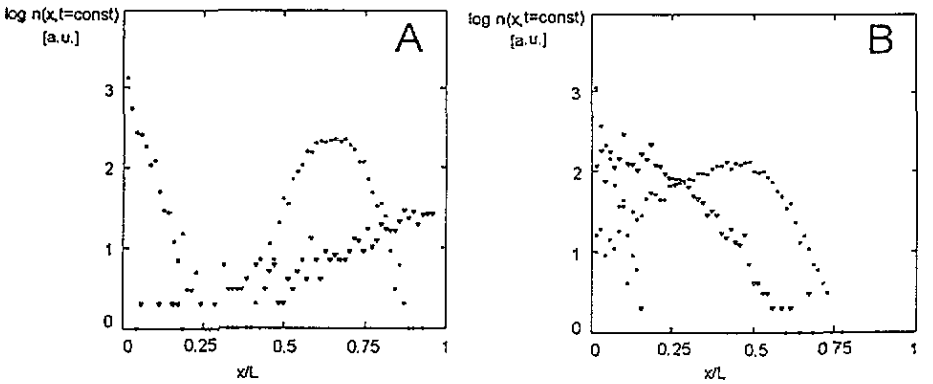

Figure 3. Spatial distributions of the carrier packets at the same time after injection, for different spatial distributions of hopping centres: ▽, $L/D = 0.0$; ●, distribution (6), $L/D = 3.0$; ○, distribution (7), $L/D = 3.0$. (A) $\sigma = 0.0kT$; (B) $\sigma = 3.5kT$. In both parts $\nu t = 10^4$ and $c = 0.2$.

currents decrease more slowly for higher L/D, so that the increasing non-uniformity acts qualitatively again like a decrease of c, and/or an increase of σ. For a higher degree of the spatial non-uniformity ($L/D \approx 3.0$), a wider half width σ of the energetic distribution ($\sigma \approx 10.0kT$), and a lower defect concentration ($c \approx 0.1$), the effective TOF is difficult to determine, the whole transient being a current decay of slope close to -1.

For total defect density increasing with x (7) the effect of the spatial non-uniformity is quite different. For short times the current profiles are even steeper than the corresponding transients in uniform systems, but at longer times after injection the rate of the current decay decreases to zero, and, for sufficiently dense systems, a sufficient value of the non-uniformity parameter (and not too wide energetic centre distribution), a current increase is observed, which reflects an exponential increase of the effective carrier packet drift velocity near the collecting contact. The occurrence of the current maxima immediately before the final current decay in a quite wide range of the parameters is the most characteristic feature of the carrier transport in the layers with total centre density increasing with x. After the effective TOF the current slopes decrease with increasing degree of non-uniformity, L/D, similarly as for distribution (6).

The comparison of the curves for the same ratio L/D and different spatial centre distributions (6) and (7) (and the same c and σ) shows thus a remarkable polarity dependence of transient currents (cf for example figure 4(C) and (D) for $\sigma = 0.0kT$, and figure 5(C) and (D) for $\sigma = 3.5kT$). Note that strong differences due to the reversed polarity occur only in the initial parts of the transients (before the effective TOF). In contrast, the slopes of the final current decay remain always linear in the log–log scale, and practically do not depend on the polarity for r–ε hopping (the final parts of curves denoted by a, b, c, and d in figure 5(C) and (D) and of curves a and b in figure 6(B) are almost exactly parallel), so the value of the non-uniformity parameter L/D changes the slope of the final current decay in the same way for both spatial distributions, (6) and (7). The dependence of the final decay slope on various parameters is shown in more detail in figure 7. The upper and two lower curves in figure 7(A) correspond to spatially uniform layers. $1 + \beta$ depends strongly on c for r hopping ($\sigma \approx 0.0kT$), and a slight polarity dependence appears (the two middle lines in figure 7(A), drawn for $L/D = 1.0$ for both polarities). For larger L/D the polarity and concentration dependence are negligible. On increasing σ the dependence of $1 + \beta$ on c

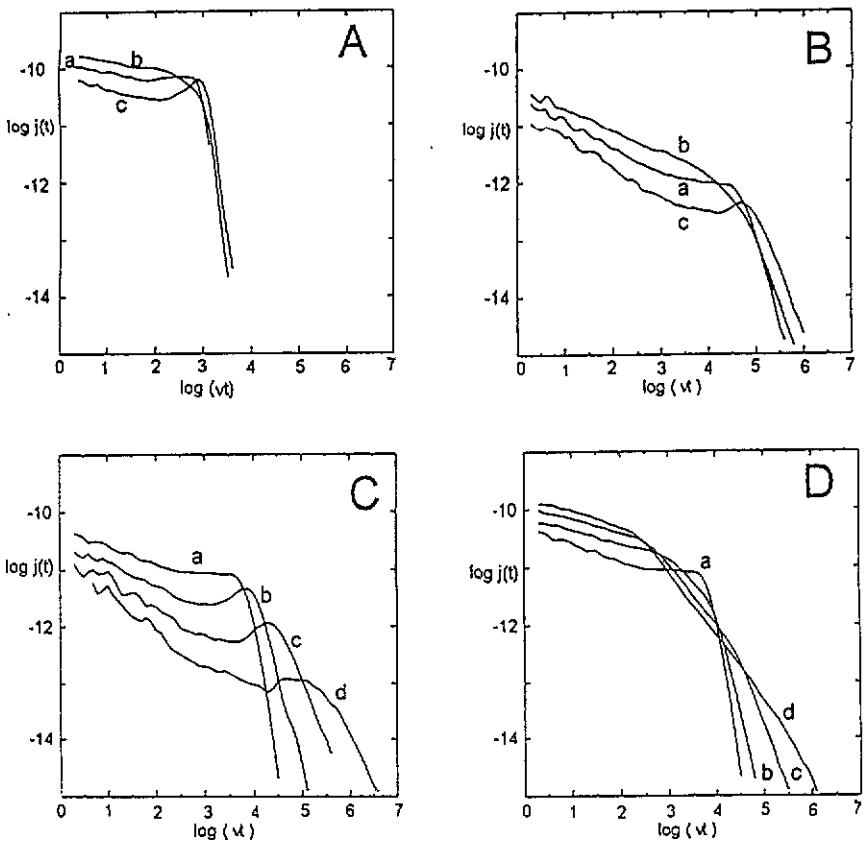

Figure 4. r hopping ($\sigma = 0.0kT$) transient currents for various centre concentrations c and various degrees of non-uniformity L/D. (A) $c = 0.5$; curve a, $L/D = 0.0$; curve b, $L/D = 1.0$, spatial distribution (6); curve c, $L/D = 1.0$, spatial distribution (7); (B) $c = 0.1$; curve a, $L/D = 0.0$; curve b, $L/D = 1.0$, spatial distribution (6); curve c, $L/D = 1.0$, spatial distribution (7); (C) $c = 0.2$, spatial distribution (7); curve a $L/D = 0.0$; curve b, $L/D = 1.0$; curve c, $L/D = 2.0$; curve d, $L/D = 3.0$; (D) $c = 0.2$, spatial distribution (6); curve a, $L/D = 0.0$; curve b, $L/D = 1.0$; curve c, $L/D = 2.0$; curve d, $L/D = 3.0$.

becomes marginal even for uniform layers, and the final slopes are not influenced by the L/D value, nor the polarity (figure 7(B) filled and empty squares for spatial distributions (6) and (7) respectively).

3.3. Spatially non-uniform layers—effective TOF and hop statistics

The effective TOF is an important characteristic of the current profiles. It is usually determined from the intersection of the straight lines tangential to the current profile before and after the change of the slope due to the arrival of the carrier packet at the collecting electrode. The values of the TOF determined in such a standard way in uniform layers are shown in figure 8(A) with empty symbols. The logarithm of TOF depends non-linearly on c, and increases strongly in the low-concentration limit. The determination of the effective TOF in not as straightforward in the case of non-uniform layers. For the current profiles that show distinct peaks we have estimated the TOFs as the intersection of the line tangential to the current at the inflection point on the left side of the maximum, and the line tangential to the final current decay. For the transients with no peaks with spatial distribution (7), and for the currents with spatial distribution (6), the TOF determination is much more arbitrary. Despite

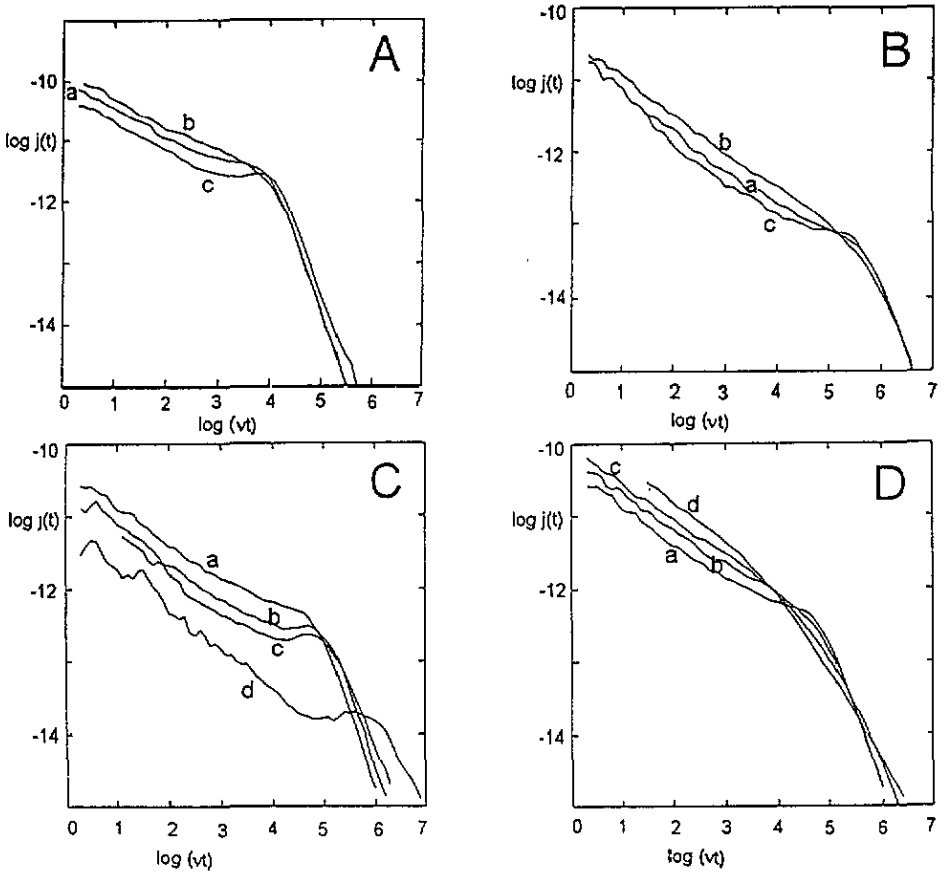

Figure 5. r–ϵ hopping transient currents with $\sigma = 3.5kT$, for various centre concentrations c and various degrees of non-uniformity L/D. (A) $c = 0.5$; curve a, $L/D = 0.0$; curve b, $L/D = 1.0$, spatial distribution (6); curve c, $L/D = 1.0$, spatial distribution (7); (B) $c = 0.1$; curve a, $L/D = 0.0$; curve b, $L/D = 1.0$, spatial distribution (6); curve c, $L/D = 1.0$, spatial distribution (7); (C) $c = 0.2$, spatial distribution (7); curve a, $L/D = 0.0$; curve b, $L/D = 1.0$; curve c, $L/D = 2.0$; curve d, $L/D = 3.0$; (D) $c = 0.2$, spatial distribution (6); curve a, $L/D = 0.0$; curve b, $L/D = 1.0$; curve c, $L/D = 2.0$; curve d, $L/D = 3.0$.

the uncertainty about the exact values, the TOFs seem to be independent of the layer polarity (the same L/D in (6) and (7)). The values marked in figure 8(A) with full symbols are the arithmetic averages of the TOF estimations with spatial centre distributions (6) and (7). As seen, the layer non-uniformity does not influence the qualitative concentration dependence of the effective TOF. The dependence of the TOF on the non-uniformity parameter L/D is shown in more detail in figure 8(B) (for various values of σ, and a given centre concentration c). For wider energetic distributions the L/D dependence of the effective TOF is negligible, whereas for narrower energetic centre distributions it remains approximately linear.

Let us finally see how the distributions of the total numbers of hops performed between $x = 0.0$ and $x = L$ are influenced by the layer non-uniformity. Figure 9 shows the corresponding histograms for various values of L/D. As is seen, increasing L/D parameter introduces generally more dispersion, similarly to increasing σ, and/or decreasing c. The widening of the distributions of total numbers of hops performed between $x = 0$ and $x = L$ due to increasing L/D, however, proceeds in a different way than that due to increasing σ and/or decreasing c. In the latter case the increase of the dispersive character of the

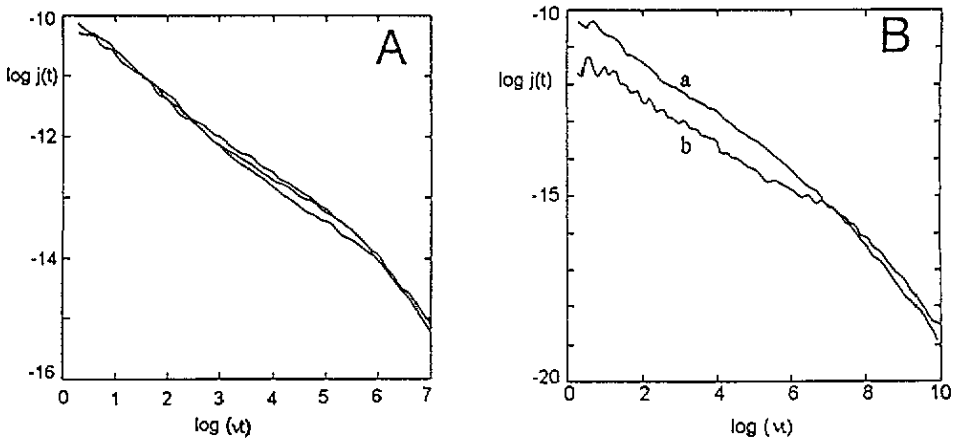

Figure 6. r–ε hopping transient currents with $\sigma = 7.0kT$, for various centre concentrations c and various degrees of non-uniformity L/D. (A) $c = 0.5$; middle curve, $L/D = 0.0$; upper curve, $L/D = 1.0$, spatial distribution (6); lower curve $L/D = 1.0$, spatial distribution (7); (B) $c = 0.1$; curve a, $L/D = 3.0$, spatial distribution (6); curve b, $L/D = 3.0$, spatial distribution (7).

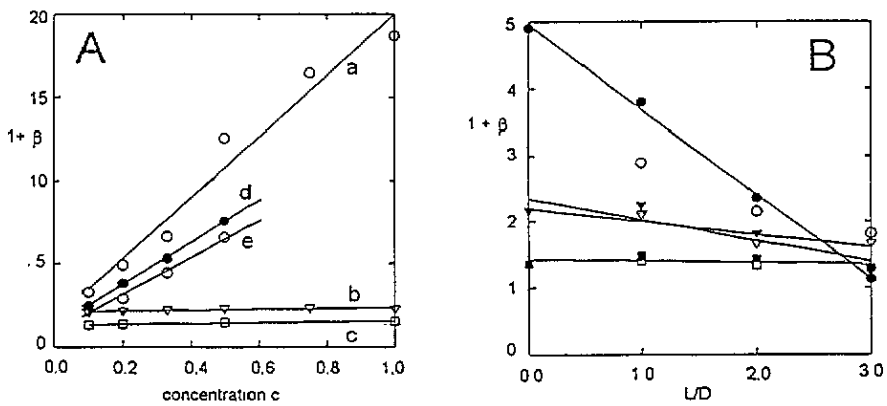

Figure 7. Final slopes $1 + \beta$ as functions of concentration c (A) and non-uniformity parameter L/D (B). (A) Curve a, $L/D = 0.0$, $\sigma = 0.0kT$; curve b, $L/D = 0.0$, $\sigma = 3.5kT$; curve c, $L/D = 0.0$, $\sigma = 7.0kT$; curve d, $L/D = 1.0$, spatial distribution (6), $\sigma = 0.0kT$; curve e, $L/D = 1.0$, spatial distribution (7), $\sigma = 0.0kT$. (B) Circles, $\sigma = 0.0kT$; triangles, $\sigma = 3.5kT$; squares, $\sigma = 7.0kT$; filled symbols, distribution (6); empty symbols, distribution (7).

currents is accompanied by the elimination of individual carrier walks with low number of jumps, and by the appearance of a monotonically decaying tail of individual walks with higher than average number of jumps (cf figure 2). As a rule, less than 0.3% of the injected carriers perform occasionally more than, say, five times the most probable number of hops. In contrast, increasing L/D does not eliminate the shortest carrier walks (figure 9), and the tail of long walks becomes a uniform distribution, extending to more than ten times the most probable number of hops. For $L/D = 3.0$ and $c = 0.1$ the tail of long walks extends uniformly up to 10^5 hops (the maximum number allowed by the length of the storage vector). Such a dependence of the distribution of the total numbers of hops on L/D originates from the superposition of the contributions from subsequent slices of the layer of various centre concentrations.

The behaviour of the characteristic features of the current profiles shows that the

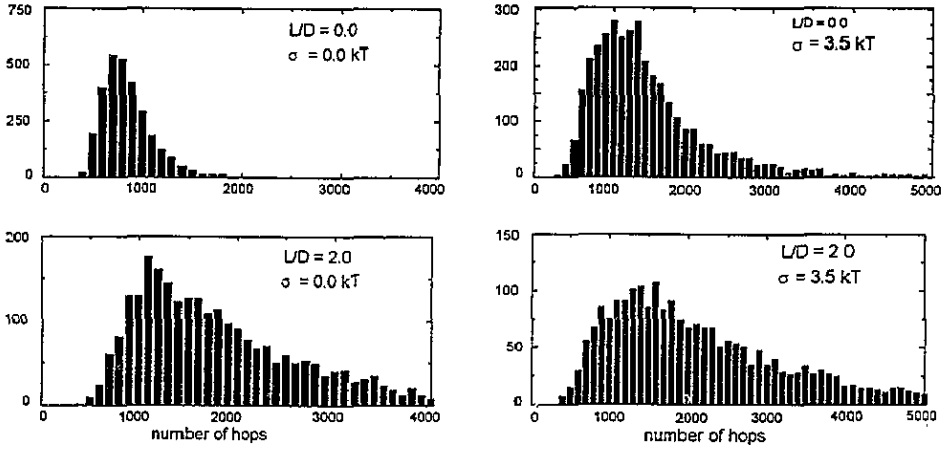

Figure 8. The effective TOF as functions of concentration c (A) and non-uniformity parameter L/D (B). Empty symbols, uniform spatial centre distribution ($L/D = 0.0$); filled symbols, non-uniform spatial distribution ($L/D = 1.0$). Circles, $\sigma = 0.0kT$; triangles, $\sigma = 3.5kT$; squares, $\sigma = 7.0kT$.

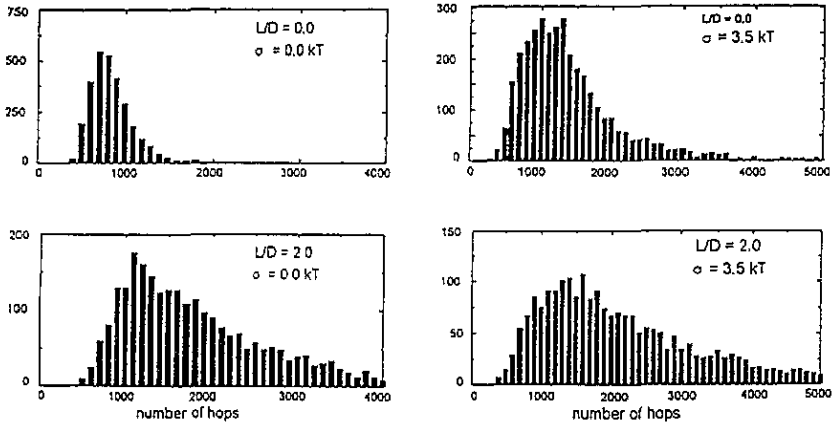

Figure 9. Histograms of the total numbers of jumps performed by the carriers between $x = 0$ and $x = L$ for $\sigma = 0.0kT$ and $\sigma = 3.5kT$ as functions of the non-uniformity parameter L/D. Hopping centre density $c = 0.2$.

dispersion originates from increasing σ, decreasing c, and increasing degree of spatial non-uniformity L/D. If a large amount of dispersion is due to a wide centre distribution in energy ($\sigma \geqslant 7.0kT$), the overall shape of the current profile, as well as the effective TOF, are hardly influenced by the spatial non-uniformity of the total centre density, independent of the presence, or lack of, positional disorder. For narrower Gaussian distributions ($2.0kT \leqslant \sigma \leqslant 5.0kT$) the effects due to the spatial non-uniformity are important, despite the low-concentration limit, where they are covered by the effects due to a significant positional disorder. With no, or low energetic disorder ($0.0kT \leqslant \sigma \leqslant 2.0kT$) the influence of the spatial non-uniformity on the current profiles is most distinct, and persist even in very dilute systems. Thus, for given c, the influence of the variations of the total hopping centre density over the layer thickness increases with increasing temperature, which reduces the σ/kT ratio.

4. Concluding remarks

Hopping transient currents measured in the classical TOF experiment are highly sensitive to the spatial macroscopic scale variations of the total centre concentration, as has been shown above for a special case of the Gaussian distribution of the centre energies. The detailed shape of the transients depends in a complicated way on the system dilution, the width of the energetic centre distribution, and the spatial variations of the total centre concentration. It should be underlined that our simulations have been performed for extremely thin layers (70 lattice constants, which for the data we used correspond to $\sim 5 \times 10^{-8}$ m), and the influence of the spatial non-uniformity on the TOF transient currents for thicker layers should be studied in future.

It seems that, even having at our disposal analytical expressions for the currents, developed for certain one- (or more) parameter families of the shape functions $S(x)$, it would be very difficult to determine univocally the spatial centre distribution from the measurement results obtainable within the TOF experiment alone. However, the qualitative results shown in the present paper suggest that the existence of the spatial non-uniformity of the layer could be recognized by the observation of the changes of the TOF current shape with increasing temperature. At higher temperatures the transients show lower dispersion due to the energetic disorder, and the characteristic features of the x-dependent total centre density, such as the polarity dependence, or the appearance of the current maxima or plateaux just before the effective TOF, become more pronounced.

Acknowledgments

This work has been sponsored by KBN, grants 2367 9102 and 2P302 16004.

References

Abkowitz M, Stolka M, Weagley R, McGrane K and Knier F 1989 *Synth. Met.* **28** C553
Adler J and Silver M 1982 *Phil. Mag.* B **45** 307
Arkhipov V I and Rudenko A I 1982 *Phil. Mag.* B **45** 189
Bassler H 1984 *Phil. Mag.* **50** 347
Bassler H, Schonherr G, Abkowitz M and Pai D M 1982 *Phil. Rev.* B **26** 3105
Di Marco P, Kalinowzski J, Giro G and Rybicki J 1989 *Thin Solid Films* **182** 271
Emoto N and Kotani M 1983 *Chem. Phys. Lett.* **101** 386
Kao K C and Hwang W 1981 *Electrical Transport in Solids* (Oxford: Pergamon)
Leal Ferreira G F 1977 *Phys. Rev.* B **16** 4719
Marshall J M 1978 *Phil. Mag.* B **38** 335
—— 1981 *Phil. Mag.* B **43** 401
—— 1983a *Rep. Prog. Phys.* **46** 1235
—— 1983b *Phil. Mag.* B **47** 323
Marshall J M, Barclay R P, Main C and Dunn C 1985 *Phil. Mag.* **52** 997
Marshall J M and Main C 1983 *Phil. Mag.* B **47** 471
Marshall J M and Sharp A C 1980 *J. Non-Cryst. Solids* **35 & 36** 99
Muller-Horsche E, Haarer D and Sher H 1987 *Phys. Rev.* B **35** 1273
Pautmeier L, Richert R and Bassler H 1989 *Phil. Mag. Lett.* **59** 325
Richert R, Pautmeier L and Bassler H 1989 *Phys. Rev. Lett.* **63** 547
Ries B and Bassler H 1987 *Phys. Rev.* B **35** 2295
Ries B, Bassler H, Grunevald M and Movaghar B 1988 *Phys. Rev.* B **37** 5508
Rudenko A I and Arkhipov V I 1982a *Phil. Mag.* B **45** 177
—— 1982b *Phil. Mag.* B **45** 209

Rybicki J and Chybicki M 1988 *J. Phys. C: Solid State Phys.* **21** 3077
—— 1989 *J. Phys.: Condens. Matter* **1** 4623
Rybicki J, Chybicki M and Feliziani S 1991a *Proc. Conf. on Molecular Crystals '91 (Łódź)* (Łódź: University of Łódź) p 123 (in Polish)
Rybicki J, Chybicki M, Feliziani S and Mancini G 1990 *J. Phys.: Condens. Matter* **2** 3547
Rybicki J, Feliziani S, Mancini G and Chybicki M 1992 *J. Phys.: Condens. Matter* **4** 3783
Rybicki J, Feliziani S, Tomaszewicz W, Jachym B and Chybicki M 1991b *J. Phys.: Condens. Matter* **3** 4229
Rybicki J, Rybicka A, Mancini G, Feliziani S and Chybicki M 1993 *J. Phys.: Condens. Matter* **5** 5027
Samoć N and Zboiński Z 1978 *Phys. Status Solidi* a **46** 251
Schein L B, Rosenberg A and Rice S L 1986 *J. Appl. Phys.* **60** 4287
Scher H and Montroll E W 1975 *Phys. Rev.* B **12** 2455
Schmidlin F 1977a *Solid State Commun.* **22** 451
—— 1977b *Phys. Rev.* B **16** 2362
Schonherr G, Eiermann R, Bassler H and Silver M 1980 *Chem. Phys.* **52** 287
Seynhaeve G, Adriaenssens G J, Michiel H and Overhof H 1988 *Phil. Mag.* B **58** 421
Tomaszewicz W, Rybicki J, Jachym B, Chybicki M and Feliziani S 1990 *J. Phys.: Condens. Matter* **2** 3311
Weissmiller J 1985 *Phil. Mag.* B **51** 349
Yuh H J and Stolka M 1988 *Phil. Mag.* B **58** 539